GeoConvention
Calgary • Canada • March 7-11 2016
OPTIMIZING RESOURCES

Gabor nonstationary deconvolution for attenuation compensation in highly lossy dispersive media

Kay Y. Liu, Elise C. Fear, and Mike E. Potter*
Department of Electrical Engineering, University of Calgary
yuliu@ucalgary.ca

Summary

Gabor nonstationary deconvolution (Margrave et al., 2011) was developed in the field of Seismology to compensate for attenuation loss, correct phase dispersion, and produce images with high resolution. Compared to seismic waves, a stronger attenuation and dispersion effect is observed in microwave frequency electromagnetic (EM) waves, especially with a propagating medium that has loss and high dispersion, such as biological tissues. In the microwave image, it is displayed as a characteristic blurriness or lack of resolution that increases with time/distance. To produce microwave images with high solution, there is a strong need for a technique that is able to compensate for energy loss and correct for wavelet distortion. Therefore, the Gabor algorithm is necessary in order to deal with the nonstationarity in EM wave propagation and attenuation.

Gabor deconvolution is essentially based on the assumption that the anelastic attenuation of seismic waves can be described by a constant Q theory (Kjartansson, 1979). Our study reveals that the same definition of Q as in seismic can also be used to characterize the EM wave propagation and attenuation. The Q for EM waves is not constant over the microwave frequency of interest; however, a new parameter Q* (Turner and Siggins, 1994), which is closely related to Q, can be approximated as constant for highly lossy dispersive biological tissues. Q and Q* might be different in the order of magnitude; however, these quantities describe the attenuation and dispersion in the same manner.

Our test results indicate that the Gabor nonstationary deconvolution is able to sufficiently compensate for attenuation loss and correct phase dispersion for EM waves that propagate through high lossy dispersive media. It can work effectively in the condition that a constant Q* is achieved.

Q characterization of EM wave propagation

In EM applications, an important parameter to quantify energy loss is the loss tangent, *tanδ*. Von Hippel (1954) associated the loss tangent with the quality factor Q to quantify the energy loss as EM waves propagate in the dielectric. He defined the Q as the inverse of the loss tangent, given by

$$Q = \varepsilon' / \varepsilon'', \tag{1}$$

where ε' and ε'' correspond to the real and the imaginary parts of the complex relative permittivity. For an electric field of amplitude E_0, (1) can be rewritten as

$$Q = 2\pi \frac{\frac{1}{2}\varepsilon_0 \varepsilon' E_0^2 / T}{\frac{1}{2}\omega \varepsilon_0 \varepsilon'' E_0^2}, \tag{2}$$

where ε_0 is equal to the permittivity of free space, ω is the angular frequency, and T is the duration of one wave cycle. Equation (2) implies that Q is the ratio between the average energy stored per half cycle and the energy dissipated per half cycle. This definition is consistent with the one in (Kjartansson, 1979, Sheriff, 1984, and Aki and Richards, 2002) for characterizing the seismic attenuation. However, it is rarely of direct use since only in special experiments is it possible to measure the stored energy. Therefore, following the differential form of (2) as in (Stacey et al., 1975), we derive the mathematical formula of Q as

$$Q = \omega/(2v\alpha). \quad (3)$$

This relation is the same as the one defined in (Aki and Richards, 2002) for seismic waves. With geological materials, the values of Q are normally in the range of [50, 300] over the seismic frequencies (Sheriff, 1984). Our calculation for a variety of biological tissues (Gabriel et al., 1996) reveals that the Q lies somewhere between 1.5 and 8 over the frequencies of microwave imaging. This is more than an order of magnitude lower than the range of values typically given for seismic Q, which indicates that wavelet dissipation and dispersion is far more pronounced in radar data than in seismic data. As well, our calculation indicates that the Q is not constant over the microwave frequencies. Fortunately, a new parameter Q* is introduced by Turner and Siggins (1994), defined as

$$Q^* = \frac{1}{2v}\left(\frac{d\alpha}{d\omega}\right)^{-1}, \quad (4)$$

where the phase velocity v is approximated as a constant value over the frequency band of radar pulse, α being the attenuation coefficient, and $d\alpha/d\omega$ the first order derivative of the attenuation coefficient with respect to the frequency. Equation (4) implies that, in the region where Q is approximately linear with frequency, a constant Q* can be approximated. Q and Q* might be different in total amplitude; however, these quantities describe the same changes in wavelet shape that occur during propagation.

Gabor nonstationary deconvolution

The changes in the waveform and bandwidth of the propagating wavelet due to the time-dependent frequency response, is called nonstationarity (Margrave et al., 2011). To account for nonstationarity, Gabor deconvolution is based on the fact that time-frequency decomposition of the recorded signal can be described by a nonstationary convolutional model in Gabor domain as

$$\hat{S}(f,\tau) \approx W(f)B(f,\tau)R(f,\tau), \quad (5)$$

where $\hat{S}(f,\tau)$ is the Gabor transform of recorded signal, $W(f)$ is the Fourier transform of the source wavelet, $B(f,\tau)$ is the Fourier transform of the attenuation function, and $R(f,\tau)$ is the Gabor transform of the reflectivity. The objective of Gabor deconvolution is solving for $R(f,\tau)$ using $\hat{S}(f,\tau)$. To achieve this objective, $B(f,\tau)$ and $W(f)$ need to be estimated based on $\hat{S}(f,\tau)$.

The attenuation function describes the impulse response of the attenuation process for any travel time τ. By estimating the attenuation function, we can remove it from the recorded signal; thus, the rest can be treated effectively by a stationary convolutional model. There are various ways to estimate the attenuation function in the Gabor domain. In particular, Margrave et al. (2002 and 2011) reported that the hyperbolic smoothing approach is robust and able to yield a more consistent estimate of the Gabor magnitude spectrum of the propagating wavelet. Hyperbolic smoothing is essentially based on the assumption that the nonstationary effects of attenuation are minimum phase and their Gabor magnitude spectra can be described by a constant Q as

$$|B(f,\tau)| = e^{(-\pi|f|\tau/Q)}. \quad (6)$$

Example

In order to assess the performance of Gabor nonstationary deconvolution in a more realistic application, reflection measurements are acquired with a real phantom (Fear et al., 2013). FIG. 1(a) shows the phantom structure. It is a dispersive homogeneous medium with effective permittivity $\varepsilon_{eff}(\omega) = 15$ and effective conductivity $\sigma_{eff}(\omega) = 0.01\ S/m$, and contains a lossless cylindrical inclusion with $\varepsilon_{eff}(\omega) = 2.08$. In order to effectively couple the microwave signal into the imaged object, the radar and the phantom were placed in a background medium with $\varepsilon_{eff}(\omega) = 2.5$ and $\sigma_{eff}(\omega) = 0.04\ S/m$. The radar position relative to the inclusion is illustrated in FIG. 1(b). During the data acquisition, the radar behaved as both transmitter and receiver, i.e., zero offset. The radar is repositioned over a cylindrical surface (in gray). Along the +*z* direction, the radar scanned through seven vertical positions from the bottom to the top of the phantom. At each vertical location, the radar rotated around the phantom and

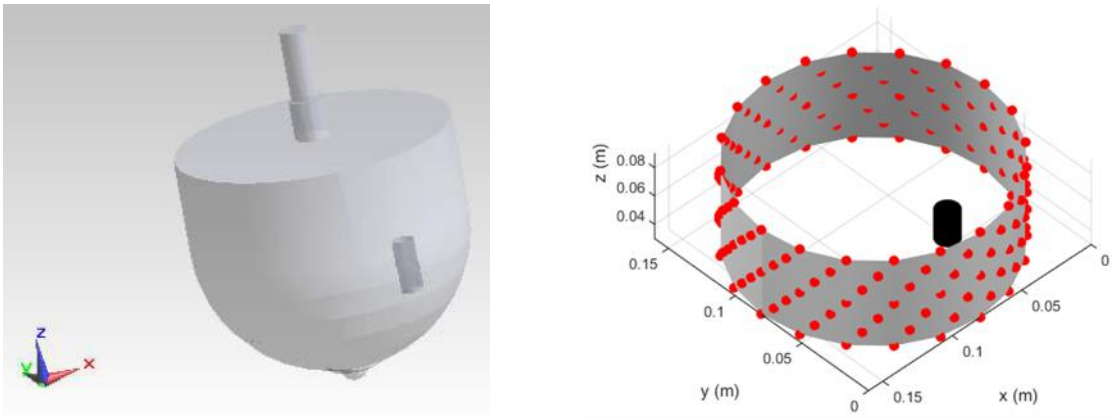

(a) (b)

FIG. 1 The phantom structure (a) and the acquisition geometry (b). The red dots represent the location of radar, and the black cylinder represents the inclusion.

collected data from 20 different locations. In total, 140 measurements were collected. Kirchhoff migration was utilized for image reconstruction.

Gabor nonstationary deconvolution and Wiener stationary deconvolution were applied to the signals prior to image formation. We compared the reconstructed images with and without deconvolution as preconditioning. The results are shown in FIG. 2. All three images can detect the existence of the object of interest (i.e., inclusion) at the accurate location. The image with Gabor deconvolution as preconditioning shows the best localization effect (i.e., the sharpness of the imaged object), while the image reconstructed with the data without deconvolution shows the least localization effect, and the image with the stationary deconvolution is in between. A slightly higher background noise may be observed in the image with Gabor deconvolution. This is because the Gabor algorithm is not able to differentiate the noise from the data. When compensating for the wave attenuation, the Gabor algorithm may also boost up the noise mixed together with the data. This noise might be reduced by applying a low pass filter to the post Gabor signal; however, there is always a tradeoff between improving the image resolution and decreasing the noise level.

Conclusions

In this study, we extended the application of Gabor nonstationary deconvolution from seismic imaging to microwave imaging. The latter involves the microwave frequency EM wave propagation in media that exhibit high loss and high dispersion. Our theoretical derivations and experimental results demonstrate that (1) the same definition of Q can be found for seismic waves and EM waves; (2) the Q for EM waves varies with frequency; however, a parameter Q* can be found by taking the first order derivative of Q over frequency, which can be approximated as a constant over the microwave frequencies of interest; and (3) Gabor nonstationary deconvolution is able to remove the wavelet dispersion in the presence of high attenuation and dispersion. However, since Gabor deconvolution is not designed to distinguish between noise and data, the algorithm may unintentionally boost up the noise when compensating for attenuation. Thus, a noise attenuation process might be necessary prior to Gabor deconvolution.

Acknowledgements

This work is financially supported by the Natural Sciences and Engineering Research Council of Canada (NSERC), the Alberta Innovates Technology Futures (AITF), NSERC Collaborative Research and Training Experience (CREATE) Program, and the University of Calgary. The authors are grateful to David Henley for sharing his understanding and insights in Gabor nonstationary deconvolution, and

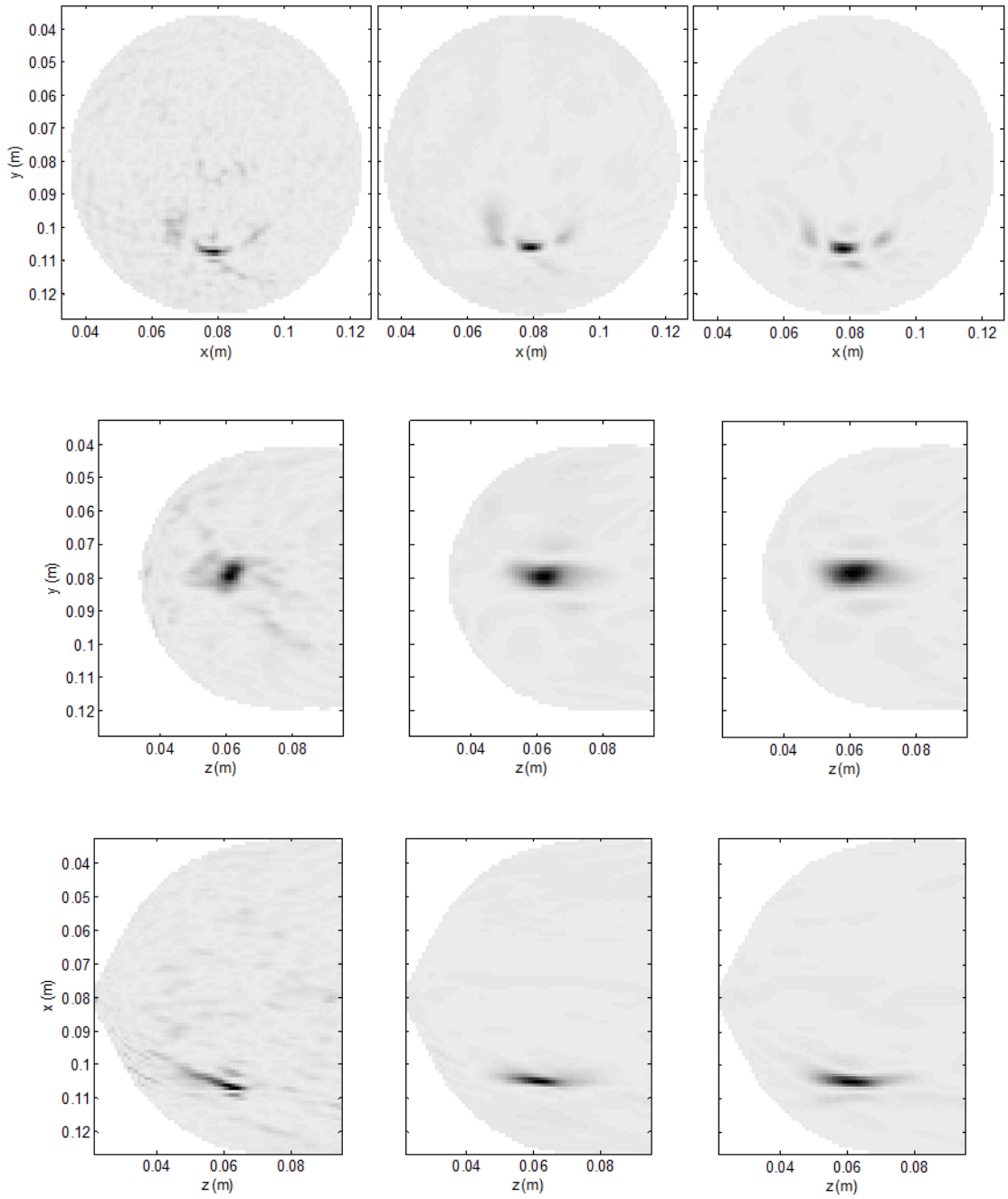

FIG. 2 Time focusing at the location of the maximum response in the image. From left to right, the images are reconstructed using Gabor nonstationary deconvolution as preconditioning, using stationary deconvolution as preconditioning, and without deconvolution. From top to bottom, the images are sliced through the xy plane, the yz plane, and the xz plane, respectively.

deeply appreciate his comments and suggestions. The authors thank Jeremie Bourqui for his help on antenna measurement systems. Finally, the authors wish to thank the Consortium for Research in Elastic Wave Exploration Seismology (CREWES) for providing the software support.

References

Aki, K., and Richards, P. G., 2002, Quantitative Seismology: Theory and methods. University Science Books.

Fear, E. C., Bourqui, J., Curtis, C., Mew, D., Docktor, B., and Romano, C., 2013, Microwave Breast Imaging With a Monostatic Radar-Based System: A Study of Application to Patients: IEEE Transaction on Microwave Theory and Techniques, 61,

Gabriel, S., Lau, R. W., and Gabriel, C., 1996, The dielectric properties of biological tissues .3. Parametric models for the dielectric spectrum of tissues: Physics in Medicine and Biology, 41, 2271-2293.

Irving, J. D., and Knight, R. J., 2003, Removal of wavelet dispersion from ground-penetrating radar data: Geophysics, 68, 960-970.

Kjartansson, E., 1979, Constant Q-wave propagation and attenuation: Journal of Geophysical Research, 84, 4737-4748.

Liu, K. Y., Fear, E., and Potter, M., 2015, Antenna aperture localization for arrival time correction using first-break: Progress In Electromagnetics Research B, *62*, 105-120.

Margrave, G. F., Henley, D. C., Lamoureux, M. P., Iliescu, V., and Grossman, J. P., 2002, A update on Gabor deconvolution: CREWES Research Report, 14.

Margrave, G. F., Dong, L., Gibson, P., Grossman, J., Henley, D., and Lamoureux, M., 2003, Gabor deconvolution: Extending Wiener's method to non-stationarity: CREWES Research Report, 15.

Margrave, G. F., Lamoureux, M. P., and Henley, D. C., 2011, Gabor deconvolution: Estimating reflectivity by nonstationary deconvolution of seismic data: Geophysics, 76, W15-W30.

Perz, M., Mewhort, L., Margrave, G. F., and Ross, L., 2005, Gabor deconvolution: Real and synthetic data experiences: CSEG Convention Expanded Abstracts.

Sheriff, R. E., 1984, Encyclopedic Dictionary of Exploration Geophysics. Society of Exploration Geophysics.

Stacey, F. D., Gladwin, M. T., McKavanagh, B., Linde, A. T., and Hastie, L. M., 1975, Anelastic damping of acoustic and seismic pulses: Geophysical Surveys, 2, 133-151.

Turner, G., and Siggins, A. F., 1994, Constant Q-attenuation of subsurface radar pulses: Geophysics, 59, 1192-1200.

Von Hippel, A. R., 1954, Dielectrics and Waves. John Wiley & Sons, Inc.